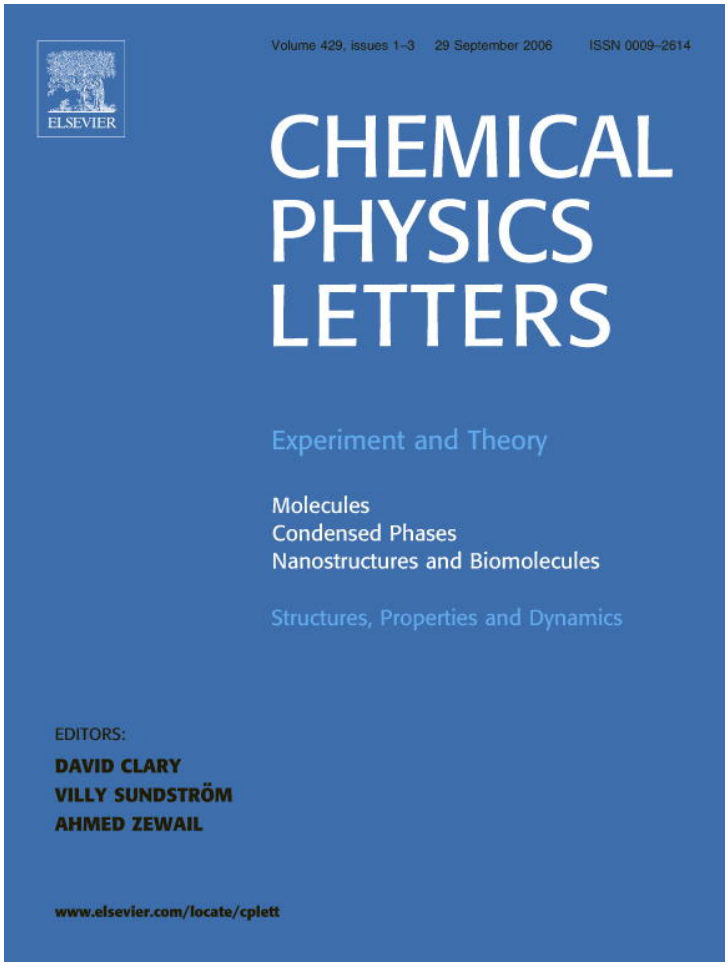

Available online at www.sciencedirect.com
ScienceDirect
Chemical Physics Letters 429 (2006) 294–298
CHEMICAL PHYSICS LETTERS
www.elsevier.com/locate/cplett

Nonlinear optics of molecular nanostructures in solution: Assessment of the size and nonlinear optical properties

Vladislav I. Shcheslavskiy [a,b,*], Solomon M. Saltiel [c], Denis A. Ivanov [d], Anatolii A. Ivanov [d], Vladislav Y. Petrusevich [e], Georgi I. Petrov [e], Vladislav V. Yakovlev [e]

[a] Optoelectronics Research Centre, University of Southampton, Southampton SO17 1BJ, UK
[b] Laboratoire d'Optique Biomédicale, Ecole Polytechnique Fédérale de Lausanne, 1015 Lausanne, Switzerland
[c] Faculty of Physics, Sofia University, 5 J. Bourchier Blvd, Sofia, BG-1164, Bulgaria
[d] Photochemistry Center of Russian Academy of Sciences, Moscow 117421, Russia
[e] Department of Physics, University of Wisconsin-Milwaukee, P.O. Box 413, Milwaukee, WI 53201, USA

Received 1 March 2006; in final form 13 July 2006
Available online 29 July 2006

Abstract

Most of the known self-assembly processes occur in solution, where nanosized objects interact each other forming new structures. Their real-time characterization in terms of the size and optical properties of these objects is vital for understanding those interactions. We report a novel application of nonlinear optics to study molecular structures and assemblies. By measuring the power of the third-harmonic generated in a solution of nanoparticles, we determined both the size and the third-order nonlinear optical susceptibility of those nanoparticles. The newly developed technique was successfully employed to observe the structural organization of collagen (type I) molecules in solution.

The theory of light scattering was launched by Lord Rayleigh [1] who provided the framework to describe light interaction with particles whose size is smaller than the wavelength of light. In 1940, Debye extended Rayleigh's theory to study molecular weights, sizes, shapes and interactions of biological molecules in solutions [2]. The later experimental and theoretical developments have led to many applications of light scatting in material science, biological imaging and aerosol sensing [3].

With the advent of ultra-short laser sources and the development of nonlinear optics, nonlinear optical effects in light scattering became increasingly important. Second- and third-order scattering processes from micron and sub-micron particles, which result, for example, in the generation of new light frequencies at the doubled and tripled frequency of the incident wave, have been studied both theoretically and experimentally [4,5]. Nonlinear optical measurements that enable high structural sensitivity [6,7] and superior spatial discrimination against the out of focus molecules [8] has been well-established. The second-harmonic (SH) is dipole-allowed only in non-centrosymmetric media, and vanishes for typical symmetric sub-wavelength structures. The third harmonic (TH), which is dipole-allowed in any material, on the other hand, vanishes in the bulk of the media due to the Gouy phase shift [9] experienced by a light beam passing through the focal plane. However, the above symmetry is broken in the presence of an interface, and a strong third-harmonic signal is generated leading to a wide variety of applications in noninvasive biomedical imaging [10,11], and material science [12,13].

We have recently discovered that, if instead of a single interface, a submicron particle is placed in the focus of the near-infrared laser beam, the generated TH signal follows a fourth power dependence on its size, when the size

* Corresponding author. Address: Laboratoire d'Optique Biomédicale, Ecole Polytechnique Fédérale de Lausanne, 1015 Lausanne, Switzerland. Fax: +41 21 6937820.
E-mail address: vladislav.shcheslavskiy@epfl.ch (V.I. Shcheslavskiy).

0009-2614/$ - see front matter © 2006 Elsevier B.V. All rights reserved.
doi:10.1016/j.cplett.2006.07.071

of a particle is greater than about 50 nm [14]. For a typical light intensity of the order of 10^{10}–10^{11} W/cm^2, this TH signal appears to be many orders of magnitude more powerful than the SH signal, and even stronger than linear light scattering.

In this report we capitalize on this intriguing finding to make measurements of the size and nonlinear optical susceptibility, $\chi^{(3)}$, to study transformational rearrangement of collagen molecules in solution.

The idea of our experiment is outlined in Fig. 1. The solution to be investigated was flowing through a transparent cell, which can be a microfluidic device as well, and the laser light is focused first on the air/glass and glass/solution interfaces and then into the bulk of the cell. The forward propagating time-integrated TH signal is collected with a high numerical aperture lens for each of the positions of the beam's focus. With the prior knowledge of all the refractive indices, and the nonlinear optical susceptibility of the glass and a pure solution, which can be measured independently before the experiment, one can derive both the size and the nonlinear optical susceptibility, $\chi^{(3)}$, of the nanostructures in solution.

We used several assumptions in our derivations. First, we neglect all the aberrations, assuming that they are not significant under moderate focusing conditions [15]. While for focusing optics with a numerical aperture (NA) more than 0.55, correction factors need to be introduced, for our particular experimental conditions, focusing conditions with NA $\leqslant 0.55$ do not require additional correction factors [16]. The Maxwell's equations for the third-harmonic wave are solved in the slow varying envelope approximation (SVEA), for which conditions are fulfilled if radiuses of particles are larger than 20 nm. The reflections from all the interfaces are taken into account by introducing corrective coefficients since the reflected wave is not considered in SVEA [14]. Finally, we assume the spherical symmetry of the object whose size is smaller than a beam waist radius, the wavelength of the incident light and the coherence length.

The ratio of powers of the third-harmonic generated on the air/glass ($P_1(3\omega)$) and glass/liquid ($P_2(3\omega)$) interfaces can be described as [13]:

$$P_2(3\omega)/P_1(3\omega) = 1 + F(n_{\text{glass}}, N_{\text{glass}}, n_{\text{liquid}}, N_{\text{liquid}}, \chi^{(3)}_{\text{glass}}, \chi^{(3)}_{\text{liquid}}), \quad (1)$$

where n_i and N_i are refractive indices at the incident and third harmonic frequency, respectively. Function $F(\ldots)$ has a rather complex form and is typically analyzed numerically [14]. When particles are present in solution, we use an effective-medium approach to get the 'effective' nonlinear susceptibility ($\chi^{(3)}_{\text{eff}}$), which can be expressed in terms the susceptibility of the pure solution itself ($\chi^{(3)}_0$) and the susceptibility of the particle ($\chi^{(3)}_{\text{particle}}$) [17]:

$$\chi^{(3)}_{\text{eff}} = (1-p)\chi^{(3)}_0 + p\chi^{(3)}_{\text{particle}}, \quad (2)$$

where p is the volume fraction of our spheres in the solution. This volume fraction is just the product of the number density of the particles and their volume.

The third-harmonic power generated from a Rayleigh particle in the index-matching liquid is given by [14]:

$$P_3(3\omega) = 1024\frac{N_{\text{liquid}}}{c^2 n^3_{\text{liquid}} w_0^6}(\Gamma_{\text{liquid}} - \Gamma_{\text{particle}})^2 R^4 P^3(\omega) K(R), \quad (3)$$

where $\Gamma_i = 3\pi^2 \frac{\chi^{(3)}_i}{\lambda_1 N_i}$; $P(\omega)$ is the power of the incident fundamental beam; w_0 is the radius of a beam waist; $K(R) = 1$, if $R \geqslant \frac{2\lambda}{\pi\alpha}$ and $K(R) = [1-\cos(\alpha/2)]/[1-\cos(\lambda/\pi R)]$, if $R \leqslant \frac{2\lambda}{\pi\alpha}$, where α is a full plane angle for collecting the TH signal, which is related to the numerical aperture (NA) of the collecting lens. Coefficient K accounts for the fact that not all TH signal is collected from the particles with sizes below some certain limit due to the limited acceptance angle of the collecting optics. As seen from Eq. (3) the third harmonic power depends on the fourth power of the microsphere diameter. This is coming from the fact that third

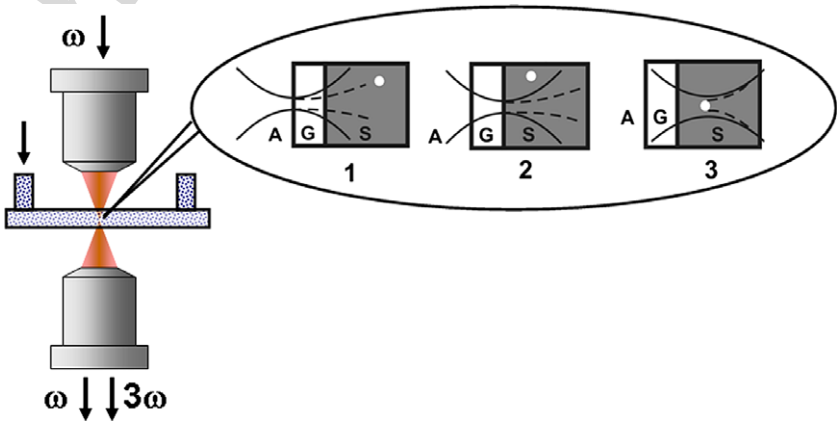

Fig. 1. Schematic of the experimental setup.

harmonic intensity generated by a focused laser beam scales as the square of the medium thickness (i.e. $\propto R^2$), while the total energy, i.e. what is detected in experiment, is proportional to particle cross section, which in its turn is proportional to πR^2 for the case of sphere shape. The area of the laser beam, which does not go through sphere's material, does not contribute to the third harmonic signal (Fig. 1). So finally, the recorded third harmonic energy will be proportional to the fourth power of the particle radius.

Knowledge of the concentration of particles which was controlled in all our experiments, enables the set of equations. (1)–(3) to be solved with respect to the radius of the particle, R, and its nonlinear susceptibility $\chi^{(3)}_{\text{particle}}$. In a more general case of non-index-matching liquid the power of the third-harmonic is expressed in a more complex form than Eq. (3), and the solution is not available analytically, but can be solved numerically.

To experimentally verify our approach, we first apply it to determine the third-order nonlinear optical susceptibilities and sizes of fused silica nanospheres (Bangslabs, Inc) with diameters ranging from 200 nm to 1000 nm. The output of a 26.5 MHz Cr:forsterite laser [18] with a wavelength of 1.26 μm, pulse duration of 40 fs and average power of 230 mW is focused with a high-numerical aperture (NA = 0.55) aspheric lens into a flowing fused silica cell, and the third-harmonic signal is collected by an aspheric lens (NA = 0.55) and redirected into the spectrometer with an attached CCD for detection. The concentration of particles in solution is kept below 10^8 cm^{-3} to ensure that on average less than one particle was present in the focal volume. Higher concentrations of particles complicate the situation due to the superimposed third harmonic signals from different particles and possible multiple scattering effects. Under typical experimental conditions (CCD acquisition time ~30 s, flow rate ~10 ml/min), we estimate about 200 particles (at concentration of 10^8 cm^{-3}) passing through the focal volume during a typical observation time interval.

We measured $\chi^{(3)}_0$ of the index-matching liquid to be $\chi^{(3)}_0 = (3.2 \pm 0.3) \cdot 10^{-14}$ esu by measuring the TH powers at the air/glass and glass/liquids interfaces and applying a well-established algorithm [13]. Using the above procedure, we obtain the values for $\chi^{(3)}_{\text{particle}}$ and the diameter presented in Figs. 2a and 2b, which shows an excellent agreement with the independently determined values. The error bars are determined by the size distribution specified by the manufacturer (10%) and the accuracy of our measurement projected on the calculated using Eqs. (1)–(3) particles' size diameter (ranging from 11% for the smallest size particles down to 8% for the largest particles).

For the next step, we apply the developed methodology to study collagen (type I) assembly in acetic acid solution. Collagen, being one of the most abundant biopolymers in living organisms provides their principal structural and mechanical support. Recently, using the hyper-Rayleigh scattering and dynamic light scattering techniques we found that collagen's first hyperpolarizability and translational diffusion coefficient undergo significant changes above a certain concentration of collagen in solution [19]. It was attributed to the formation of supramolecular aggregates (globules) of collagen. This intermediate phase precedes the formation of cholesteric structures of collagen, which mimic the assembly of this protein in real tissues [20]. It is reasonable to expect variations of molecular hyperpolarizability and the size of nanoassembly across the transformation.

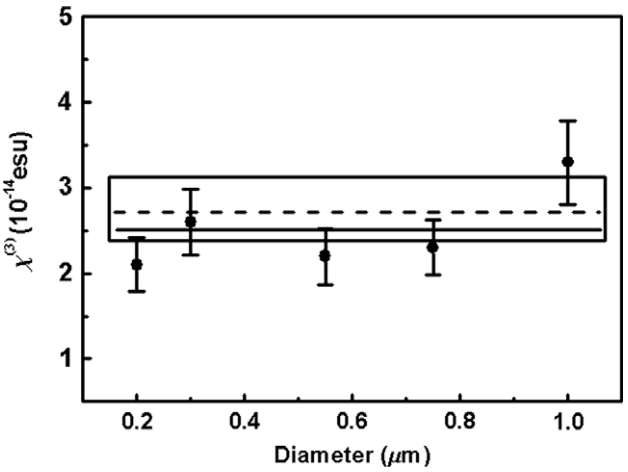

Fig. 2a. The third-order nonlinear susceptibility as a function of the diameter of fused silica particles. The dashed line and the solid rectangle represent the averaged literature data and the standard deviation for $\chi^{(3)}$ of fused silica.

The above derivations were based on the assumption of a spherical shape, while collagen molecule looks more like a cylinder (with a diameter and length of 1.5 nm and 300 nm, respectively) and more rigorous theoretical treatment is needed to accurately describe TH from such a structure. In the simplest possible approach, one can treat collagen molecules as spheres. This approach is widely used in light scattering, where a cylindrically shaped object is approximated with a prolate ellipsoid, having the same length and volume as a cylinder. The effective hydrodynamic radius of a prolate ellipsoid has been considered by Tanford [21] who evaluated the case of ellipsoids with a high axial ratio. A rod of length 300 nm and diameter 1.5 nm would have a hydrodynamic radius of 26 nm. We should note that introduction of hydrodynamic radius implies that the assemblies do not interact with each other or have a week interaction. Since the data acquisition time is much less than the time required for molecules to assemble, one can essentially neglect the intermolecular interaction on this time scale.

An alternative approach does not alter the geometry of assembly, but assumes that those molecular assemblies are very thin in diameter and very long in length. In this case, the method of independent dipoles [22] can be used, and the total TH scattering power should be proportional to the square of the total dipole moment. Since the total dipole moment will be scaled as R^2, the generated TH power will be scaled as R^4, i.e. the same way as in the

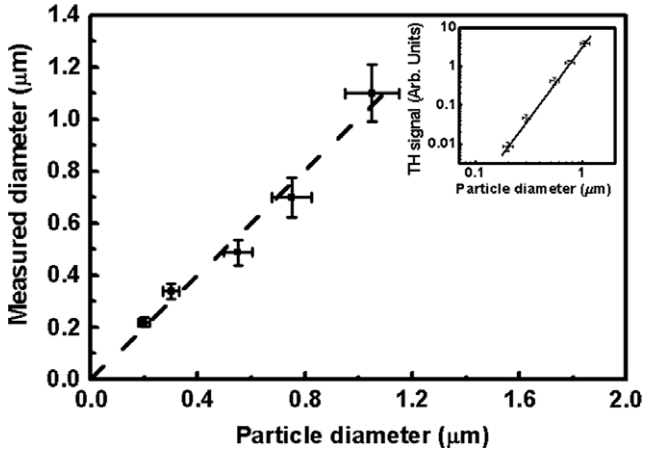

Fig. 2b. The measured size of fused silica spheres plotted against the size specified by manufacturer with 10% size distribution shown as a horizontal error bar. The dashed line shows ideal 1:1 correspondence. Inset: fourth-power dependence of TH signal on sizes of spheres. Inset: fourth-power dependence of TH signal on sizes of spheres. Inset: fourth power dependence of relative third harmonic signal vs diameters of the spheres.

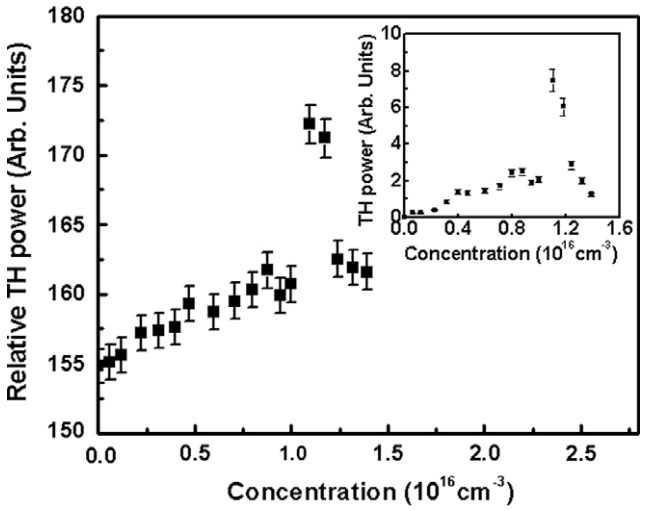

Fig. 3. The power of the TH generated on the glass/solution interface and in the bulk (inset) of the solution with respect to the TH power generated on the air/glass interface as a function of the collagen concentration in solution.

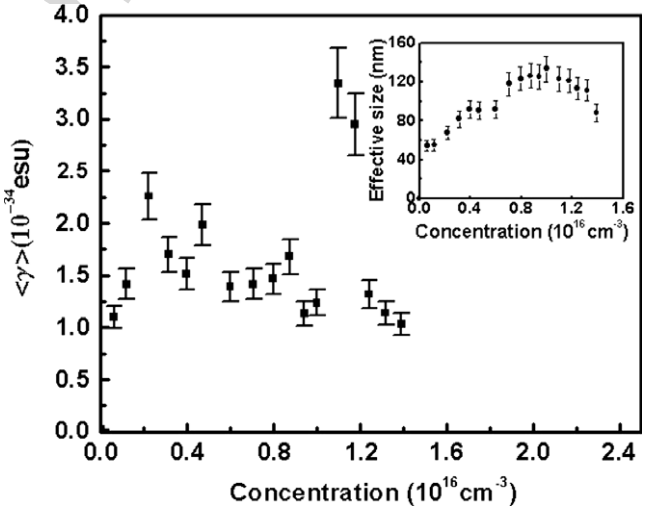

Fig. 4. The measured value of orientationally averaged second hyperpolarizability and the effective size of collagen supramolecular assemblies as a function of collagen concentration in solution.

Eq. (3) with the only difference being that in the later case R is the radius of a sphere, while here it is the radius of a cylinder. However, in both cases it represents the characteristic size of a molecular assembly. While both of these approaches consider extreme geometries of molecular assemblies, the final result is about the same and the characteristic dimension of the system will be different by some factor, which can be, in principle, measured for a well-calibrated system. To make analysis simpler, we will limit ourselves to a simplified spherical model and will try to evaluate the variation of the characteristic size of assemblies as a function of their concentration in solution.

It is important to mention, however, that the developed method will be ideal for globular proteins such as albumin and globulin.

Collagen type I is obtained from calf skin and supplied by ICN biomedicals. We dissolve the protein in 0.04 M acetic acid solution with a concentration of 10 mg/ml. The mixture was stirred with a magnetic stirrer, centrifuged and filtered with a syringe filter (0.45 μm). Gel electrophoresis confirmed the purity of collagen. The stock solution was kept at 4 °C and used for adding to pure 0.04 M acetic acid solution in experiments. The pH of the solution was maintained at 4.8. All measurements were done at 20 °C.

The experimental results are shown in Fig. 3, where TH signals generated on the glass/solution interface and in the bulk of the solution are plotted as a function of the collagen concentration. Using the earlier developed theory we calculate the second hyperpolarizability (γ) of collagen and its size as a function of concentration assuming the refractive index of collagen to be 1.41 [23]. These results are presented in Fig. 4 and show a dramatic increase of the second hyperpolarizability at the collagen concentration of $1.1 \times 10^{16}\,\mathrm{cm}^{-3}$. Such a strong enhancement of hyperpolarizability can be explained in terms of highly polar character of the formed collagen assemblies [24]. Although the concentration of collagen molecules is high and may lead to the presence of more than one molecule in the focal region (which may seem contradictive to the theoretical model), we make a measurement not of a single molecule but of an averaged value of size and hyperpolarisability of molecular aggregates.

The later drop in the second hyperpolarizability at still higher number densities of collagen molecules is attributed to the process of pre-cholesteric globules formation. The effective size of collagen molecular assembles first gradually increases from about 50 nm to 140 nm, and then drops to about 80 nm at the highest concentrations. The lowest measured effective radius is 50 nm, which is in a close

agreement with the effective hydrodynamic radius of collagen molecules, approximated by a prolate ellipsoid. Although the understanding of structure-property relationships for the third-order nonlinear optical effects is limited, all microscopic theoretical models predict a large non-resonant third-order optical nonlinearity associated with delocalized π-electron systems [24]. That means that for the precholesteric phase, the extent of delocalization of π-electrons is probably reduced. However, additional experiments are required to check this hypothesis which is beyond the scope of the work.

In summary, we have demonstrated a novel application of nonlinear optics to study molecular assemblies. The ability to detect and characterize nanostructures may find application in correlated spectroscopy based on the third-harmonic imaging, which compared to a commonly used fluorescence correlation spectroscopy [25] utilizes a natural ability of any nano-structure to generate light at the frequency of the third harmonic. For example, this technique can be very useful for characterization of viruses and bacteria spores [26]. Their sizes and internal structure strongly influence their resistance to disinfectant chemicals [27]. Also this technique may find potential applications in studying of macromolecular complexes at nanoscale and monitoring the processing of pharmaceutical nanoparticles. Finally, the knowledge of nonlinear optical properties and sizes of nanoobjects is important in biosensor applications [28] and studying protein interactions [29].

References

[1] J.W. Strut (Lord Rayleigh), Philos. Mag. 41 (1871) 107.
[2] P. Debye, Ann. Phys. 46 (1915) 809.
[3] F. Bohren, D.R. Huffman, Absorption and Scattering of Light by Small Particles, Wiley, New York, 1983.
[4] J.I. Dadap, J. Shan, K.B. Eisenthal, T.F. Heinz, Phys. Rev. Lett. 83 (1999) 4045.
[5] J. Kasparian et al., Phys. Rev. Lett. 78 (1997) 2952.
[6] Y.R. Shen, Proc. Natl. Acad. Sci., USA 93 (1996) 12104.
[7] T. Verbiest et al., Science 282 (1998) 913.
[8] W. Denk, J.H. Strickler, W. Webb, Science 248 (1990) 73.
[9] L.G. Gouy, Compt. Rendue Acad. Sci., Paris 110 (1890) 1251.
[10] J. Squier, M. Muller, J. Brakenhoff, K. Wilson, Opt. Express 3 (1998) 315.
[11] D. Yelin, Y. Silberberg, Opt. Express 5 (1999) 169.
[12] R. Barille, L. Canioni, L. Sarger, G. Rivoire, Phys. Rev. E 66 (2002). Art. No. 067602.
[13] V.I. Shcheslavskiy, G. Petrov, V.V. Yakovlev, Appl. Phys. Lett. 82 (2003) 3982.
[14] V.I. Shcheslavskiy, S.M. Saltiel, A. Faustov, G.I. Petrov, V.V. Yakovlev, J. Opt. Soc. Am. B 22 (2005) 2402.
[15] S.W. Hell, G. Reiner, C. Cremer, E.H.K. Stelzer, J. Microsc. 169 (1993) 391.
[16] R. Pillai, G. Brakenhoff, M. Mueller, Opt. Express 14 (2006) 260.
[17] D. Stroud, V. Wood, J. Opt. Soc. B 6 (1989) 778.
[18] V.I. Shcheslavskiy, V.V. Yakovlev, A.A. Ivanov, Opt. Lett. 26 (2001) 999.
[19] V.I. Shcheslavskiy, G.I. Petrov, V.V. Yakovelv, Chem. Phys. Lett. 402 (2005) 170.
[20] M.M. Giraud-Gullie, Biol. Cell 67 (1989) 97.
[21] C. Tanford, Physical Chemistry of Macromolecules, Wiley, New York, 1961.
[22] E.D. Purcell, C.R. Pennypacker, Astrophys. J. 186 (1973) 705.
[23] D.W. Leonard, K.M. Meek, Biophys. J. 72 (1997) 1382.
[24] P. Prasad, D. Williams, Introduction to Nonlinear Optical Effects in Molecules and Polymers, J. Wiley& Sons, Inc., 1991.
[25] D. Magde, W. Webb, E. Elson, Phys. Rev. Lett. 29 (1972) 705.
[26] G.I. Petrov, V.V. Yakovlev, A.V. Sokolov, M.O. Scully, Opt. Express 13 (2005) 9537.
[27] J.Y. Maillard, Rev. Med. Microbiol. 12 (2001) 63.
[28] A.J. Haes, R.P. van Duyne, J. Am. Chem. Soc. 124 (2002) 10596.
[29] W.L. Connors, J. Heino, J. Anal. Biochem. 337 (2005) 246.